

# **Analysis of oxytactic microorganisms and magnetic dipole for radiative Cross fluid flow configured by nano-enhanced phase materials**

Muhammad Tabrez<sup>a</sup>, Waqar Azeem Khan<sup>a,1</sup>, Muhammad Irfan<sup>b</sup>, Iftikhar Hussain<sup>a</sup> and Taseer

Muhammad<sup>c</sup>

<sup>a</sup>Department of Mathematics, Mohi-ud-Din Islamic University, Nerian Sharif, Azad Jammu and Kashmir 12010, Pakistan

<sup>b</sup>Department of Mathematical Sciences Federal Urdu University of Arts, Sciences & Technology, Islamabad 44000, Pakistan

<sup>c</sup>Department of Mathematics, College of Science, King Khalid University, Abha, Saudi Arabia

**Abstract:** Nanotechnology took interest of research community for the reason that of its vast range of uses and applications like killing cancerous cell, preparation of medicines, nano-robot technology, manufacturing of modern aircraft, distillation process of water, biomedical engineering, thermal storage as well as transfer system, cooling of electronic devices, aircraft engines, power plants, coolants in nuclear reactors, construction industry etc. Here the Concept of microorganism is utilized to make suspension more stable and nano sized particles are used with the effect of bio-convection. Major purpose behind this investigation is exploration of two dimensional Cross fluid flow of ferrofluid with magnetic dipole effects. Moreover important features of Brownian motion along with thermophoresis parameters are computed for Cross model having effects of magnetism termed as ferrofluid with consideration of important characteristics like convective conditions on boundary motile microorganisms, as well as thermal gradients all are under consideration. Here, PDEs are converted into sets of ODEs and solved via bvp4c method. Results showed that temperature of ferrofluid increases with increase in

---

<sup>1</sup>[waqarazeem@bit.edu.cn](mailto:waqarazeem@bit.edu.cn); [Waqar\\_qau85@yahoo.com](mailto:Waqar_qau85@yahoo.com)

parameter of thermophoresis as well as thermal effects, which results in reduction of Prandtl number. The process of microorganism reduces for higher values of Peclet number.

**Keywords:** Ferromagnetic Cross fluid, Thermal radiation, Magnetic dipole, Bio convection and Viscous dissipation.

## 1. Introduction

The choice of liquid functioning medium is crucial to the performance of the whole system. Water is an appropriate heat transfer fluid due to its lower cost, better heat capacity as well as no toxicity, but water can only absorb 13% of its energy, and water results in some problems like freezing, rust as well as corrosion. Improving the efficiency of thermal systems has many benefits, such as reduced environmental impact, reduced energy utilization and reduction in costs. In recent decades, nanofluids have been evaluated economically and environmentally according to sustainability approaches to determine their utility in thermal systems and they are suggested as an alternative solution of many challenges must be overcome before nanofluids can become a viable technology so, nanofluids can be produced in thermal states with positive economic and environmental outcomes. Nanofluids have been investigated as an innovative fluid to improve the profitability and efficiency of various thermal systems used in industries, residential as well as commercial purposes. Due to their unique thermo physical properties and many applications in important fields such as refrigeration, electronics, transportation of energy, seawater desalination, engine cooling, aerospace technology, electronic cooling, solar energy applications, vehicles engines working, polymer processing, solar collector, nuclear refrigeration, lubrication systems, microprocessors, energy production, cooling towers in industries, heat exchanger, hyperthermia, biomedical engineering, automation, targeted drug delivery, biomedicine, etc. Fascinatingly, nanofluids are also used in the food industry for preparation of different foods. Because of the mass transfer characteristics of nanofluids, their

use is common for crystallization, extraction as well as distillation, which is possible because the nanoparticles higher surface area that leads to several mechanisms that play a role in enhancing or worsening the mass transfer capabilities of nanofluids. In automotive radiator technology, a small quantity of nanoparticles that are suspended inside desired base fluid results in cooling and dissipation of heat at a much higher rate as compared to a surplus of common base fluid excluding nanoparticles, hence radiator can be smaller in size that saves costs as well as space and weight. Advances in nanotechnology have greatly contributed to solving main problems in the field of engineering and medical, the adaptability of nanofluids is mainly attributed to the shape, size, ionic composition as well as type of nanoparticles. The pursuit of thermal cooling performance for enhanced heat dissipation has never been greater across technologies, particularly for thermal applications in electronics, solar systems, and electric motors along with manufacturing technologies. Therefore, the trend of cooling technologies having excellent thermal properties without loss is increasing day by day; nanofluids have great potential to fulfill these growing demand refs [1-12].

To reduce the emission of carbon dioxide it is highly recommended to promote nonrenewable energy and discover its more sources. Scientists are interested in research on natural assets as well as sustainable energy for the purpose of lowering carbon dioxide emission, which is beneficial for the environment as it causes a reduction of air pollution. Growth in the economy of the world promotes nonrenewable forms of energy while rising prices of crude oil results in promotion of renewable forms of energy. In developed countries policy makers suggest to reduce use of nonrenewable energy and recommend emphasizing on promotion of renewable energy. Climate change as well as global warming is among basic issues of this century, since change in climate directly results in global warming, pollution in our environment, along with results in emission of greenhouse gases. Hence a shifting is needed from fossil fuels energy which causes higher carbon dioxide toward renewable energy which results in a lower economy of CO<sub>2</sub>. Since the majority of energy consumption in the world is non-renewable and its immediate shifting toward renewable is not possible, researchers are trying to reduce emission of carbon by some

suitable changes and enhancement in both forms of energy due to increasing population and technological advancements. Scholars recommended that by preferring the use of renewable energy consumption so we may reduce the impacts of climate change for human beings along with other habitants on the earth, so from 1990 this shifting of energy starts in developed countries which is promoting day by day. Transformation of non-renewable to renewable as well as other alternatives is mainly due to four reasons. Development of technology results in reduction of energy costs, support of policy makers and governments due to benefits in form of taxes, issues of climate change as cause of more greenhouse gases is another main reason, last but not least reason is instability in prices of crude oil due to increasing demand of energy and shortage of fossil fuels in future compelled the researchers to alternate sources of energy. In this modern era, almost all countries of the world are facing many challenges at the same time like health emergencies, declination of biodiversity, crises of food, and serious issues of climate change, where the wellbeing of this planet is associated with the health and welfare of humanity. Despite of the existing literature that tendency in promotion of renewable form of energy is on peak for developed or stable countries, till now domination of non-renewable energy is found over renewable energy, literature survey showed that till now consumption of non-renewable energy is more than 94 percent of total energy consumption in world main reason of this alarming fact is higher cost for investment of renewable energy. Solar energy is one of the best alternate sources of energy which is both environmentally friendly as well as the most abundant source of energy for this globe. It is also recommended by researchers to emphasize the policy makers to give better packages by governments of countries to promote renewable energies; this may include relaxation in taxes or by providing funds to organizations that are promoting renewable energies. For instance, various non-Newtonian studies dealing with the aspects of current research were explored in refs [13-23].

Major purpose behind present research is scrutinizing the arithmetical modeling for Cross model by flow of nanofluid along with effects of ferromagnetism. Here thermal radiation along with

viscous dissipation is also considered. The deficiency of naturally existing resources for energy as well as increasing pollution are two of major problems so researchers are on the point of view of usage of nanofluid as an innovative fluid that can save energy and also they are an environmentally friendly fluid. Additionally the present study has novelty literature revealed that no major contribution upon our title was found in existing literature. Here we considered Cross nanofluids flow having ferromagnetic particles, moreover we compute transfer of mass and heat during flow. The system of nonlinear PDEs are converted into nonlinear ODEs by use of fitting boundary conditions, moreover solutions of these ODEs are made possible by using a well-known scheme called bvp4c. The outcomes of obtained leading non dimensional quantities are plotted while results are discussed in detail.

## 2. Statement

In the present research problem a two-dimensional non-Newtonian steady flow of Cross fluids with ferromagnetic effects along with microorganism's insertion. The region surrounded by fluid bears subsequent restriction  $y > 0$  along with an elastic sheet along  $x$  coordinate of the plane and having the velocity with mathematical representation  $(u = ax)$ , where 'a' is a non-negative number. Under consideration magnetic field is of sufficient strength which is normal to the flow direction on dispassion that is lower to  $x$  coordinate surface but middle upon vertical coordinate shown in [Fig.1]. Moreover, Buongiorno model is considered by using thermophoresis parameter, random diffusive behavior, bioconvection, for Cross ferrofluid. The association for motile, concentration as well as ambient temperature are mathematically represented as  $N_w = N, C_w = C, T_w = T$ . The problem is modeled in the form of following nonlinear equations [24, 25 and 26].

$$\frac{\partial u}{\partial x} + \frac{\partial v}{\partial y} = 0, \quad (1)$$

$$u \frac{\partial u}{\partial x} + v \frac{\partial u}{\partial y} = \nu \frac{\partial^2 u}{\partial y^2} \left[ \frac{1}{1 + \left( \Gamma \frac{\partial u}{\partial y} \right)^n} \right] + \frac{\partial}{\partial y} \left[ \frac{1}{1 + \left( \Gamma \frac{\partial u}{\partial y} \right)^n} \right] \frac{\partial u}{\partial y} + \frac{\lambda_0}{\rho} M \frac{\partial H}{\partial x}, \quad (2)$$

$$u \frac{\partial T}{\partial x} + v \frac{\partial T}{\partial y} + \left\{ \frac{\lambda_0 T}{(\rho c)_f} \right\} \left( \frac{\partial M}{\partial T} \right) \left( u \frac{\partial H}{\partial x} + v \frac{\partial H}{\partial y} \right) = \frac{\nu}{c_f} \left[ \frac{1}{1 + \left( \Gamma \frac{\partial u}{\partial y} \right)^n} \right] \left( \frac{\partial u}{\partial y} \right)^2 \quad (3)$$

$$+ \left\{ \frac{\kappa}{(\rho c)_f} \right\} \frac{\partial^2 T}{\partial y^2} - \frac{1}{(\rho c)_f} \frac{\partial q_r}{\partial y} + \frac{(\rho c)_s}{(\rho c)_f} \left\{ D_B \frac{\partial C}{\partial y} \frac{\partial T}{\partial y} + \frac{D_T}{T_\infty} \left( \frac{\partial T}{\partial y} \right)^2 \right\},$$

$$u \frac{\partial C}{\partial x} + v \frac{\partial C}{\partial y} = \frac{D_T}{T_\infty} \frac{\partial^2 T}{\partial y^2} + D_B \frac{\partial^2 C}{\partial y^2}, \quad (4)$$

$$u \frac{\partial N}{\partial x} + v \frac{\partial N}{\partial y} = D_m \frac{\partial^2 N}{\partial y^2} - \frac{bW_c}{(C_w - C_\infty)} \left[ \frac{\partial}{\partial y} \left( N \frac{\partial C}{\partial y} \right) \right], \quad (5)$$

with

$$u = ax, v = 0, T = T_w, C = C_w, N = N_w \text{ when } y = 0, \quad (6)$$

$$u = 0, T \rightarrow T_\infty, C \rightarrow C_\infty, N \rightarrow N_\infty \text{ as } y \rightarrow \infty. \quad (7)$$

## 2.1. Modeling for magnetic field

The flow analysis of Cross ferro-nanofluid which is affected by the magnetic dipole due to appliance of magnetic field, whose  $(\Phi_1)$  (magnetic potential) is given by

$$\Phi_1 = \left( \frac{\chi_1}{2\pi} \right) \left[ \frac{x}{x^2 + (y + \alpha_1)^2} \right], \quad (8)$$

in components form  $(\Phi_1)$  is defined as

$$H_x = -\frac{\partial \Phi_1}{\partial x} = \left( \frac{\chi_1}{2\pi} \right) \left[ \frac{(x)^2 - (y + \alpha_1)^2}{\left[ (x)^2 + (y + \alpha_1)^2 \right]^2} \right], \quad (9)$$

$$H_y = -\frac{\partial \Phi_1}{\partial y} = \left( \frac{\chi_1}{2\pi} \right) \left[ \frac{2x(y + \alpha_1)}{\left[ x^2 + (y + \alpha_1)^2 \right]^2} \right], \quad (10)$$

subsequently magnetic body force and gradient of magnitude of  $H$  are proportional to each other, we have

$$H = \sqrt{\left( \frac{\partial \Phi_1}{\partial x} \right)^2 + \left( \frac{\partial \Phi_1}{\partial y} \right)^2}, \quad (11)$$

one has

$$\frac{\partial H}{\partial x} = -\left( \frac{\chi_1}{2\pi} \right) \left[ \frac{2x}{(y + \alpha_1)^4} \right], \quad (12)$$

$$\frac{\partial H}{\partial y} = \left( \frac{\chi_1}{2\pi} \right) \left[ -\frac{2}{(y + \alpha_1)^3} + \frac{4x^2}{(y + \alpha_1)^5} \right]. \quad (13)$$

Mathematical relation for the variation of  $M$  through  $T$  is given by

$$M = K(T_\infty - T), \quad (14)$$

### 3. Solution procedure

Considering

$$\begin{aligned}
\eta &= y \sqrt{\frac{c\rho}{\mu_0}}, \quad u = \frac{\partial \psi}{\partial y} = axf'(\eta), \quad v = -\frac{\partial \psi}{\partial x} = -\sqrt{\frac{c\mu_0}{\rho}} f(\eta), \\
\psi(\xi, \eta) &= \frac{\mu_0}{\rho} \xi f(\eta), \\
\theta(\eta) &= \frac{T - T_\infty}{T_w - T_\infty}, \quad \theta(\eta) = \theta_1(\eta) + \xi^2 \theta_2(\eta), \\
\varphi(\eta) &= \frac{C - C_\infty}{C_w - C_\infty}, \quad \phi(\eta) = \phi_1(\eta) + \xi^2 \phi_2(\eta), \\
\chi(\eta) &= \frac{N - N_\infty}{N_w - N_\infty}, \quad \chi(\eta) = \chi_1(\eta) + \xi^2 \chi_2(\eta).
\end{aligned} \tag{15}$$

We have

$$\left[1 + (1-n)(Wef'' )^n\right] f''' - \left[1 + (Wef'' )^n\right]^2 \left[(f')^2 - ff''\right] - \frac{2\beta\theta_1}{(\eta + \alpha)^4} = 0, \tag{16}$$

$$(1 + Rd)\theta_1'' - \text{Pr} N_b \theta_1' \phi_1' - \text{Pr} N_t \theta_1'^2 + \text{Pr} f \theta_1' + 2\lambda\beta(\theta_1 - \varepsilon) \frac{f}{(\eta + \alpha)^3} = 0, \tag{17}$$

$$\begin{aligned}
&(1 + Rd)\theta_2'' + \text{Pr} \left[ f \theta_2' - 2f' \theta_2 \right] - \lambda\beta(\theta_1 - \varepsilon) \left[ \frac{2f'}{(\eta + \alpha)^4} + \frac{4f}{(\eta + \alpha)^5} \right] + \\
&2\lambda\beta \frac{\theta_2 f}{(\eta + \alpha)^3} - \lambda \left[ \frac{1}{1 + (Wef'' )^n} \right] f''^2 - \text{Pr} N_b \left[ \phi_2' \theta_1' + \theta_2' \phi_1' \right] = 0,
\end{aligned} \tag{18}$$

$$\phi_1'' + \frac{N_t}{N_b} \theta_1'' - Scf' \phi_1' + Scf \phi_1' = 0, \tag{19}$$

$$\phi_2'' + \frac{N_t}{N_b} \theta_2'' - 3Scf' \phi_2' + Scf \phi_2' = 0, \tag{20}$$

$$\chi_1'' - Pe \left[ \chi_1' \phi_1' + \chi_1 \phi_1'' + \delta_1 \phi_1'' \right] + L_b f \chi_1' = 0, \tag{21}$$

$$\chi_2'' - Pe \left( \chi_1' \phi_2' + \chi_1 \phi_2'' + \chi_2 \phi_1' + \delta_1 \phi_2'' \right) \left( \frac{1}{1 - Pe} \right) - 2L_b \chi_2 + L_b f \chi_2' = 0, \tag{22}$$



$$\begin{aligned} \theta_1(0) = 1, \theta_2(0) = 0, \phi_1(0) = 1, f'(0) = 1, \\ \phi_2(0) = 0, \chi_1(0) = 1, \chi_2(0) = 0, \end{aligned} \quad (23)$$

$$\begin{aligned} f'(\infty) \rightarrow 0, \theta_1(\infty) \rightarrow 0, \theta_2(\infty) \rightarrow 0, \phi_1(\infty) \rightarrow 0, \\ \phi_2(\infty) \rightarrow 0, \chi_1(\infty) \rightarrow 0, \chi_2(\infty) \rightarrow 0. \end{aligned} \quad (24)$$

## 4. Declaration of curiosity

### 4.1. Friction at stretched surface

One has

$$C_{fx} = \frac{2\mu_0}{\rho_f u^2} \left[ \frac{\frac{\partial u}{\partial y}}{1 + \left( \Gamma \frac{\partial u}{\partial y} \right)^n} \right]_{y=0} \quad (25)$$

non-dimensional version

$$C_{fx} \text{Re}_x^{1/2} = \frac{2f''(0)}{1 + \{Wef''(0)\}^n}. \quad (26)$$

### 4.2. Nusselt number

We write

$$Nu_x = -\frac{x}{(T_w - T_\infty)} \left( \frac{\partial T}{\partial y} \right)_{y=0} - \frac{x}{k(T_w - T_\infty)} \frac{16T_\infty^3 \sigma^*}{3k^*} \left( \frac{\partial T}{\partial y} \right)_{y=0}, \quad (27)$$

One has

$$Nu_x \text{Re}_x^{-1/2} = -\left[ \theta_1'(0) + \xi^2 \theta_2'(0) \right] [1 + R_d]. \quad (28)$$

$$\begin{aligned}
Nu_x &= -\frac{x}{(T_w - T_\infty)} \left( \frac{\partial T}{\partial y} \right) \Big|_{y=0} - \frac{x}{k(T_w - T_\infty)} \frac{16T_\infty^3 \sigma^*}{3k^*} \left( \frac{\partial T}{\partial y} \right) \Big|_{y=0}, Sh_x = -\frac{x}{(C_w - C_\infty)} \left( \frac{\partial C}{\partial y} \right) \Big|_{y=0}, \\
C_{fx} &= \frac{\mu_0}{\rho u^2} \left[ \frac{\partial u}{\partial y} + \frac{We}{2} \left( \frac{\partial u}{\partial y} \right)^2 \right] \Big|_{y=0}, N_n = -\frac{x}{(N_w - N_\infty)} \left( \frac{\partial N}{\partial y} \right) \Big|_{y=0},
\end{aligned} \tag{26}$$

### 4.3. Sherwood number

Mathematically, it is given by

$$Sh_x = -\frac{x}{(C_w - C_\infty)} \left( \frac{\partial C}{\partial y} \right) \Big|_{y=0}, \tag{29}$$

we can find

$$Sh_x Re_x^{-1/2} = -\left[ \phi_1'(0) + \xi^2 \phi_2'(0) \right]. \tag{30}$$

### 4.4. Motile number

It is expressed as

$$N_n = -\frac{x}{(N_w - N_\infty)} \left( \frac{\partial N}{\partial y} \right) \Big|_{y=0}, \tag{31}$$

$$N_n Re_x^{-1/2} = -\left[ \chi_1'(0) + \xi^2 \chi_2'(0) \right]. \tag{32}$$

where  $Re_x = \left( \frac{xu}{\nu} \right)$ .

## 5. Results and discussion

In the present article, the mathematical simulation is proficient for the investigation of non-Newtonian Cross ferrofluid over an elastic sheet. The MATLAB technique `bvp4c` is basically a numeric scheme of finite difference, which is utilized in amalgamation along shooting technique. The impacts of non-dimensional physical parameters also involved nonlinear differential equations upon velocity, heat, mass transfer and motile movement of microorganisms. The impact of various parameters upon (MHD) ferrofluid flow with magnetic dipole is expressed by

means of graphical representations whereas we expressed the microorganism density, Sherwood number as well as Nusselt number in tabular form for better understanding of relationship.

### **Velocity Field ( $f'(\eta)$ ):**

The impacts of dimensionless parameter of fluid on velocity field are represented by means of Fig. 2(a). An increment for estimations of  $\alpha$  like ( $\alpha = 0.70, 0.75, 0.80, 0.85$ ) basis to augment the velocity of ferrofluid. Here these dimensionless parameters of fluid are important and directly influence the effects for flow of fluid. Fig. 2(b) demonstrates the decreasing behavior of ( $f'(\eta)$ ) on escalation in the estimations of power law index [ $n$ ]. Inclination in [ $n$ ] declines velocity gradient of Cross ferrofluid. It is revealed from substantial fact of prospect that existence of magnetic field attracts the fluid particles and increases fluid viscosity which acts as delaying factor on velocity of fluid and consequently ( $f'(\eta)$ ) declines.

### **Temperature profile ( $\theta_1(\eta), \theta_2(\eta)$ ):**

A deep observation for effects of [ $Pr$ ] along with Brownian motion parameter [ $N_b$ ] upon temperature  $\theta_1(\eta)$  is displayed with the assistance of Figs. 3(a,b). Since first figure illustrates the impression of [ $Pr$ ] against temperature profile [ $\theta_1(\eta)$ ]. It is concluded for rising [ $Pr$ ] has directly influences temperature of fluid and causes a decrement in fluid temperature. Second part of Fig.3 represented the path followed by ferrofluid temperature  $\theta_1(\eta)$  when [ $N_b$ ] rises, the figure shows that temperature of ferrofluid is enhanced by rising in Brownian motion symbolized as ( $N_b = 0.1, 1.1, 2.1, 3.1$ ). Since striking rate of base fluid to ferro particles increases with increase in [ $N_b$ ], consequently this higher collision rate of result in increase of heat transmission

rate so temperature increases. The performance of radiation parameter  $[Rd]$  and thermophoresis parameter  $[N_t]$  against  $[\theta_1(\eta)]$  is expressed by using Figs .4 (a, b). First part of figure shows the impacts of  $\theta_1(\eta)$  under the influence of  $[Rd]$ . An increment in the estimations of  $[Rd]$  increases the temperature profile. The effect of  $[N_t]$  is scrutinized in Fig. 4 (b). For greater estimations of thermophoresis parameter ( $N_t = 0.5, 1.5, 2.5, 3.5$ ) temperature gradient  $[\theta_1(\eta)]$  shows enhancement. Results showed that for higher  $[N_t]$  results in upsurge of thermophoretic force consequently motion of fluid particles toward lower level of energy is observed so results in inclination of fluid temperature. The performance of thermophoresis parameter  $[N_t]$  and Curie temperature  $[\varepsilon]$  on temperature  $[\theta_2(\eta)]$  is depicted with help of Fig.5 (a, b). Outcome of  $[N_t]$  on  $\theta_2(\eta)$  is explored in Fig. 5 (a). It is examined that  $[N_t]$  is boosting the  $\theta_2(\eta)$  and thickness of thermal boundary layer for ferrofluid. Fig. 5(b) is anticipated to demonstrate the presentation of  $[\varepsilon]$  on  $\theta_2(\eta)$ . The ferrofluid particles showed an imperative part for rising in transportation of heat for Cross ferrofluid.

Special effects of radiation parameter denoted by  $[Rd]$  along with Brownian motion  $[N_b]$  on temperature of fluid denoted as  $\theta_2(\eta)$  are clarified by using Figs. 6(a, b). First part of this figure is used to understand the variation in  $\theta_2(\eta)$  against rising  $[Rd]$ . It is seen from mathematical point of view that thermal radiation  $[Rd]$  is directly proportional to temperature of ferrofluid at infinity. Accordingly, as estimations of  $[Rd]$  are augmented, the temperature of Cross fluid rises. Thus, as an outcome, the temperature of ferrofluid boosted. Fig.6 (b) depicts the trajectories

of ferrofluid temperature profile  $\theta_2(\eta)$  with the increment  $[N_b]$ , the particular figure represents change in temperature of Cross ferrofluid which shows prominent increase with rise in Brownian motion.

**Concentration profile  $[\varphi_1(\eta), \varphi_2(\eta)]$ :**

The change of Schmidt number  $[Sc]$  beside thermophoresis parameter  $[N_t]$  for concentration profile  $\varphi_1(\eta)$  is expressed with Figs .7 (a, b). First portion of this figure represents the change in concentration field by variation in  $(Sc = 0.4, 0.5, 0.7, 0.9)$  and this relationship is found contrary. The relationship between Schmidt number to mass diffusivity is totally converse means rise in one quantity causes a proportional fall of other one, so results in reduction of thermal boundary layer with concentration. Second part of this figure denotes the variation in thermophoresis parameter for  $\varphi_1(\eta)$ , with rise in  $[N_t]$  causes increment of thermophoretic force so as a result more transport of the nano particles from particular area contain higher temperature toward lower one so finally concentration of fluid raises.

The effects of Brownian motion that are represented as  $[N_b]$  along with parameter of thermophoresis symbolized as  $[N_t]$  with change in concentration of fluid is expressed by using figs .8 (a, b). Initial part of figure reflects the performance of  $[N_b]$  with change in ferrofluid concentration represented as  $\varphi_2(\eta)$ . Results clarified that for higher Brownian motion the ferrofluid concentration  $\varphi_2(\eta)$  displays the declining enactment. Physically, an upsurge for estimations of  $[N_b]$  results in ascending of ferrofluid rate particles for the base fluid results in random motion having variable velocities. This movement of ferrofluid particles enhances the

transference of heat so results in declining behavior of concentration profile. It is examined from Fig. (8) b that concentration profile  $\phi_2(\eta)$  is enhanced via thermophoretic force.

### **Microorganism profile $[\chi_1(\eta), \chi_2(\eta)]$ :**

The variation of microorganisms profile with change in Lewis number along with Peclet number is articulated with the aid of Figs. 9(a,b) . When we increase  $[L_b]$  results in reduction of microorganisms profile, by means of fig. 9(b) displays a decline for the thickness of the motile micro-organisms by increasing the values  $[Pe]$  termed as Peclet number. We can better understand the importance of the  $[\delta_1]$  along with Lewis number  $[L_b]$  over the motile gyrotatic microorganism of the ferrofluid that is expressed with the help of Figs. 10 (a, b). First part of this figure represents the change in ferrofluid motile gyrotatic microorganism for higher bioconvection motile function expressed by symbol  $[\delta_1]$  . Second part of figure exposed the implication of bio-convection Lewis number  $[L_b]$  on microorganism phenomena for flow of ferrofluid. It is shown in figure that the ferrofluid microorganism phenomena declines because of rise in Lewis number. With increment in  $[L_b]$  values, diffusion in microorganisms is reduced, so caused reduction of microorganism's phenomena.

### **5.1. Features of heat-mass transfer rates and surface drag force**

The effects of different important parameters over Nusselt number while given fixed values for the rest of parameters and to analyze the results. When we increase  $(\lambda)$  denotes the viscous dissipation results in variation of dimensionless form of temperature, for minor variation in  $(Pr)$  weak thermal diffusion of ferrofluid is observed, hence consequently producing a comparatively

thin boundary layer is observed thermally. Aspects of  $\varepsilon_1, \beta, N_b$  and  $N_t$  against  $\text{Re}^{-\frac{1}{2}} \text{Nu}_x$  shown by using the first **Table**. It is perceived from the expressed tabular form that rate of thermal transference increases with greater inputs of  $N_t, N_b$  while  $\text{Re}^{-\frac{1}{2}} \text{Nu}_x$  declines against  $\varepsilon_1$ . It is also examined from tabular form **Table 2** that rate of transportation for mass declines with higher estimations of  $Sc$  along with  $N_b$  while it intensifies for greater  $N_t$ . Furthermore, it is seen in **Table 3** that  $N_n \text{Re}_x^{-1/2}$  intensifies for upsurge in  $\delta_1$  while it dwindles via greater  $L_b$ .

## 6. Conclusions

Recent research reveals the importance of nanotechnology with its applications moreover it paid much concentration upon uses of renewable energies and recommended to give preference to renewable energies over nonrenewable with wide range of its applications and keeping in view the future threats of scarcity of natural resources as well as global warming and its harmful effects. The researchers found that the trend of renewable energies like solar energy is on peak but still it covers less than 15 percent of total energy demand so policy makers' should pay attention to this serious issue. In this article we have made mathematical computations of bio-convective flow of nonlinear Cross ferrofluid in the presence of radiation phenomena that is passing over the stretching surface which has novelty as this work was not done before it. The motile microorganism phenomena along with magnetic dipole effects taken in consideration, here concept of microorganisms are used to obtain stability of small sized particles by the process of bioconvection. Basic theme of recent work is to control the phenomena of momentum along thermal boundaries by use of magnetic dipole effect. Since current investigation has a major role upon moisture migration procedures as well as vapor's diffusion, electronic along with liquescent diffusion phenomena. The basic results of this investigation are;

- With variation of non-dimensional fluid function ( $\alpha$ ), heightened the ferrofluid velocity of Cross model but this velocity is noted diminishing behavior because of power law index ( $n$ ) .
- Temperature profile of Cross ferrofluid showed increasing behavior for Brownian motion parameter ( $N_b$ ) as well as parameter of thermal radiation denoted by ( $Rd$ ) whereas the rising Prandtl number denoted by symbol ( $Pr$ ) along with curie temperature shown by ( $\varepsilon$ ) results in reduction of temperature for ferrofluid.
- With rise in Schmidt number denoted by ( $Sc$ ) the concentration of ferrofluid declines
- With rise in Peclet number ( $Pe$ ) as well as bioconvection number symbolized as ( $L_b$ ) results in lack of motile microorganism of the Cross ferrofluid.
- The increase in Nusselt number is found with increase in radiation parameter ( $Rd$ ) and Brownian motion parameter ( $N_b$ ) while it shows decreasing behavior for Prandtl number ( $Pr$ ) and Curie temperature ( $\varepsilon$ ).

**Acknowledgment:** The authors extend their appreciation to the Deanship of Scientific Research at King Khalid University, Abha, Saudi Arabia for funding this work through Large Groups Project under grant number RGP.2/329/44.

## References

1. Choi, S.U.S. and Eastman, J.A. ‘Enhancing thermal conductivity of fluids with nanoparticles’, Argonne National Lab.(ANL), Argonne, IL (United States), 1995.
2. Lu, G., Wang, X.D. and Duan, Y.Y. ‘A critical review of dynamic wetting by complex fluids: from Newtonian fluids to non-Newtonian fluids and nanofluids’, Adv Colloid



Interface Sci., 236, 43-62 (2016).

3. Amani, M., Amani, M.P.O. and Estellé, P. "Multi-objective optimization of thermophysical properties of eco-friendly organic nanofluids", J Clean Prod. 166, 350-59 (2017).
4. Khan, W.A., Irfan, M., Khan, M., et al. "Impact of chemical processes on magneto nanoparticle for the generalized Burgers fluid", J. Molecular Liquids, 234 (2017) 201-208.
5. Nikolov, A. Wu, P. and Wasan, D. "Structure and stability of nanofluid films wetting solids, an overview", Adv Colloid Interface Sci., 264, 1-10 (2019).
6. Shen, C., Lv, G., Wei, S., et al. "Investigating the performance of a novel solar lighting/heating system using spectrum-sensitive nanofluids", Appl. Energy, 270, (2020).
7. Chamkha, A.J., Mansour, M.A., Rashad, A.M., et al. "Magnetohydrodynamic mixed convection and entropy analysis of nanofluid in gamma-shaped porous cavity", J. Thermophysics Heat Transf., <https://doi.org/10.2514/1.T5983> (2020).
8. Mahian, O., Bellos, E., Markides, C.N., et al. "Recent advances in using nanofluids in renewable energy systems and the environmental implications of their uptake", Nano Energy, 86, 1-28 (2021).
9. Irfan, M. "Influence of thermophoretic diffusion of nanoparticles with Joule heating in flow of Maxwell nanofluid", Numerical Methods Partial Differential Eq., <https://doi.org/10.1002/num.22920>, (2022).
10. Anjum, N., Khan, W.A., Hobiny, A., et al. "Numerical analysis for thermal performance of modified Eyring Powell nanofluid flow subject to activation energy and bioconvection dynamic", Case Studies Thermal Eng., 39, 102427 (2022).
11. Chamkha, A.J., Armaghani, T., Mansour, M.A., et al. "MHD Convection of an Al<sub>2</sub>O<sub>3</sub>-Cu/Water Hybrid Nanofluid in an Inclined Porous Cavity with Internal Heat Generation/Absorption", Iranian J. Chemistry Chemical Eng., 41, 241635 (2022).
12. Hussain, I., Hobiny, A., Irfan, M., et al. "Impact of magnetic dipole contribution on radiative ferromagnetic Cross nanofluid with viscous dissipation aspects", J. Magnetism Magnetic Materials, 579, 170706 (2023).
13. Choi, S.U.S., Zhang, Z.G., Yu, W., et al. "Anomalous thermal conductivity enhancement in nanotube suspensions", Appl Phys Lett, 79, 2252-2254 (2001).

14. Falsafi M., and Kargarsharifabad, H., ‘‘Numerical Study of Ferrofluid Forced Convection Heat Transfer in Tube with Magnetic Field’’, *J. Comput. Methods. Eng.*, 34, 11-25 (2015).
15. Alper, A., and Oguz, O., ‘‘The role of renewable energy consumption in economic growth: Evidence from asymmetric causality’’, *Renew Sustain Energy Rev*, 60, 953-959 (2016),.
16. Bahmani A. and Kargarsharifabad, H. ‘‘Laminar natural convection of power-law fluids over a horizontal heated flat plate’’, *Heat Transf. Asian Res.*, <https://doi.org/10.1002/htj.21420> (2019).
17. Bahmani A., and Kargarsharifabad, H., ‘‘Magnetohydrodynamic free convection of non-Newtonian power-law fluids over a uniformly heated horizontal plate’’, *Ther. Science*, 24, 1323-1334 (2020).
18. Bahmani A., and Kargarsharifabad, H., ‘‘New Integral Solutions for Magnetohydrodynamic Free Convection of Power-Law Fluids Over a Horizontal Plate’’, *Iranian J. Sci. Tech., Transactions Mechanical Eng.*, 45, 1091-1101 (2020).
19. Bhatti, M.M., Öztop, H.F., Ellahi, R., et al. ‘‘Insight into the investigation of diamond (C) and Silica (SiO<sub>2</sub>) nanoparticles suspended in water-based hybrid nanofluid with application in solar collector’’, *J. Mol. Liq.*, 357 (2022).
20. Sivakumar, N., Tarakaramu, N., Narayan, P.V.S., et al. ‘‘Three dimensional magnetohydrodynamic casson fluid flow over a linear stretching surface: A numerical analysis’’, *AIP Conf. Proc.*, 2516, 170022 (2022).
21. Kargarsharifabad, H., ‘‘Optimization of arrangement of conducting fins and insulated obstacles inside a cavity: the couple of numerical solutions and genetic algorithm methods’’, *J. Ther. Analysis Calorimetry*, 147, 421–433 (2022).
22. Anwar, M.S., Hussain, M., Hussain, Z., et al. ‘‘Clay base cementitious nanofluid flow subjected to Newtonian heating’’, *Int. J. Modern Physics B*, 37, 2350140 (2023).
23. Ahmad, A., Anjum, N., Shahid, H., et al. ‘‘Impact of Darcy-Forchheimer-Brinkmann model on generalized Eyring Powell liquids subject to Cattaneo-Christov double diffusion aspects’’, *Int. J. Modern Physics B*, 37, 2350173 (2023).
24. Hussain, Z., Khan, W.A., Azam, M., et al. ‘‘Stratified thermosolutal aspects in magnetized

3D tangent hyperbolic nanofluid flow contained oxytactic moment microorganisms'', Tribol. Int., 189, 108949 (2023).

25. Hussain, Z., Khan, W.A., Ali, M., et al. ''Chemically reactive magneto-bioconvection 3D flow of radiative williamson nanofluid containing oxytactic moment of microorganisms'', Tribol. Int., 189, 108934 (2023).

26. Hussain, I. Khan, W.A., Tabrez, M., et al. ''Bioconvection aspects in magnetized Eyring-Powell fluid configured by suspension of ferromagnetic nanoparticles subject to gyrotactic moment of microorganisms'', Tribol. Int., 189, 108876 (2023).

---

## Biographies

**Muhammad Tabrez** Ph.D student in the Department of Mathematics, Mohi Ud Din Islamic University (MIU), Nerian Sharif. A.J.K, Pakistan. His current research interests in Fluid Mechanics.

**Waqar Azeem Khan** is an Assistant professor at Mohi Ud Din Islamic University (MIU), Nerian Sharif, A.J.K, Pakistan. He received PhD in Mathematics, Quaid-i-Azam University, Islamabad, Pakistan. His research interests included is Fluid Mechanics. His published 200 research articles appear in reputable international journals.

**Muhammad Irfan** is an Assistant professor at Federal Urdu University of Arts Sciences and Technology, Islamabad, Pakistan. He received PhD degree in Mathematics in the field of Fluid Mechanics, Quaid-i-Azam University Islamabad, Pakistan. His research interests included is Fluid Mechanics and published 110 research articles appear in reputable international journals.

**Iftikhar Hussain** Ph.D student in the Department of Mathematics, Mohi Ud Din Islamic University (MIU), Nerian Sharif. A.J.K, Pakistan. His current research interests in Fluid

Mechanics.

**Taseer Muhammad** is an Assistant professor at Department of Mathematics, College of Science, King Khalid University, Abha, Saudi Arabia. He received PhD in Mathematics, Quaid-i-Azam University, Islamabad, Pakistan. His research interests included is Fluid Mechanics. His published research articles appear in reputable international journals.

<b>Nomenclature</b>			
$f'$	Non dimensional velocity profile	$T$	fluid temperature
$x, y$	plane coordinate axis	$Re_x$	Local Reynolds number
$T_\infty$	Ambient temperature	$N$	Motile gyrotactic microorganism
$\lambda$	viscous dissipation parameter	$D_T$	thermophoresis diffusion coefficient
$D_T$	Thermophoresis diffusion coefficient	$\Gamma$	Material constant
$Rd$	Thermal radiation parameter	$\eta$	Non dimensional variable
$T_w$	wall temperature	$\delta_1$	Motile bioconvective difference parameter
$n$	Power law index	$N_\infty$	Ambient motile organism density
$C$	fluid concentration profile	$(\theta_1, \theta_2)$	Non dimensional temperature
$H$	Magnetic field strength	$C_w$	concentration onelastic sheet surface
$C_\infty$	Ambient concentration	$C_{fx}$	skin fraction
$\nu$	kinematic viscosity	$\alpha$	dimensionless distance
$Nu_x$	Nusselt number	$(\chi_1, \chi_2)$	Bio convection profiles
$D_B$	Brownian diffusion coefficient	$Sc$	Schmidt number

$k$	Thermal conductivity	$L_b$	Bioconvection Lewis number
$N_b$	Brownian movement parameter	$(\phi_1, \phi_2)$	Non dimensional concentration
$N_w$	Motile gyrotactic microorganism of surface	$N_t$	Thermophoresis parameter
$\varepsilon$	Curie temperature	$C_p$	Specific heat capacity
$We$	Weissenberg number	$M$	magnetic parameter
$\lambda_0$	Magnetic permeability	$u, v$	velocity components
<b>Pr</b>	Prandtl number	$Sh_x$	Local Sherwood number
$\beta$	ferromagnetic interaction parameter	$Pe$	Bio convection Peclet number

## List of Tables

**Table 1:**  $Re^{-\frac{1}{2}} Nu_x$  via various  $\varepsilon, Rd, Pr$  and  $N_t$ .

**Table 2:**  $Re^{-\frac{1}{2}} Sh_x$  against  $N_t, N_b$  and  $Sc$ .

**Table 3:**  $N_n Re_x^{-1/2}$  versus  $L_b, Pe$  and  $\delta_1$ .

## List of figures

Fig. 1: Systematic Diagram.

Figs. 2(a, b) Outcome of diverse values of  $[\alpha]$  and power law index  $[n]$  on  $f'(\eta)$ .

Figs. 3(a, b) characteristics of  $[Pr]$  and  $[N_b]$  on  $\theta_1(\eta)$ .

Figs. 4(a, b) impression of dissimilar estimations of  $[Rd]$  and  $[N_t]$  against  $\theta_1(\eta)$ .

Figs. 5 (a, b) Impact of different values of  $[N_t]$  and  $[\varepsilon]$  on  $\theta_2(\eta)$ .

Figs. 6(a, b) Aspects of different values of  $[Rd]$  and  $[N_b]$  against  $\theta_2(\eta)$ .

Figs. 7 (a, b) influence of diverse effectd  $[Sc]$  and  $[N_t]$  on  $\varphi_1(\eta)$ .

Figs. 8 (a, b) impact of different  $[N_b]$  and  $[N_t]$  on  $\varphi_2(\eta)$ .

Figs. 9 (a, b) Consequences of  $[Pe]$  and  $[L_b]$  on  $\chi_1(\eta)$ .

Figs. 10 (a, b) Consequences of  $[Pe]$  and  $[\delta_1]$  on  $[\chi_2(\eta)]$ .

## List of Tables

**Table 1:**  $Re^{-\frac{1}{2}} Nu_x$  via various  $\varepsilon, Rd, Pr$  and  $N_t$ .

$\varepsilon$	$Rd$	$Pr$	$N_t$	<b>Bvp4c</b>
0.7	0.5	0.7	0.3	0.664274
0.1				0.653243
0.5				0.644149
0.9				0.622475
1.3	0.7			0.674526
	0.9			0.681324
	1.1			0.694361
	1.3			0.708267
		1.0		0.641882
		1.2		0.638315
		1.5		0.632314

		1.7		0.628741
			2.1	0.543495
			2.4	0.551342
			2.7	0.559395
			3.0	0.562323

**Table 2:**  $\text{Re}^{-\frac{1}{2}} Sh_x$  against  $N_t, N_b$  and  $Sc$ .

$N_t$	$N_b$	$Sc$	<b>Bvp4c</b>
0.1	0.3	0.5	0.485282
0.6			0.492529
1.1			0.498715
1.6			0.501393
0.2	0.10		0.401611
	0.11		0.394532
	0.12		0.391344
	0.13		0.387154
		0.6	0.492612
		0.7	0.481539
		0.8	0.476764
		0.9	0.462325

**Table 3:**  $N_n \text{Re}_x^{-1/2}$  versus  $L_b, Pe$  and  $\delta_1$ .

$p_e$	$L_b$	$\delta_1$	<b>Bvp4c</b>
0.2	0.1	0.3	0.706356
0.3			0.698475
0.4			0.692491
0.5			0.685652
0.7	0.1		0.805392

	0.3		0.802189
	0.5		0.792155
	0.7		0.790238
		0.2	0.762325
		0.4	0.774913
		0.6	0.786327
		0.8	0.791276

### List of figures

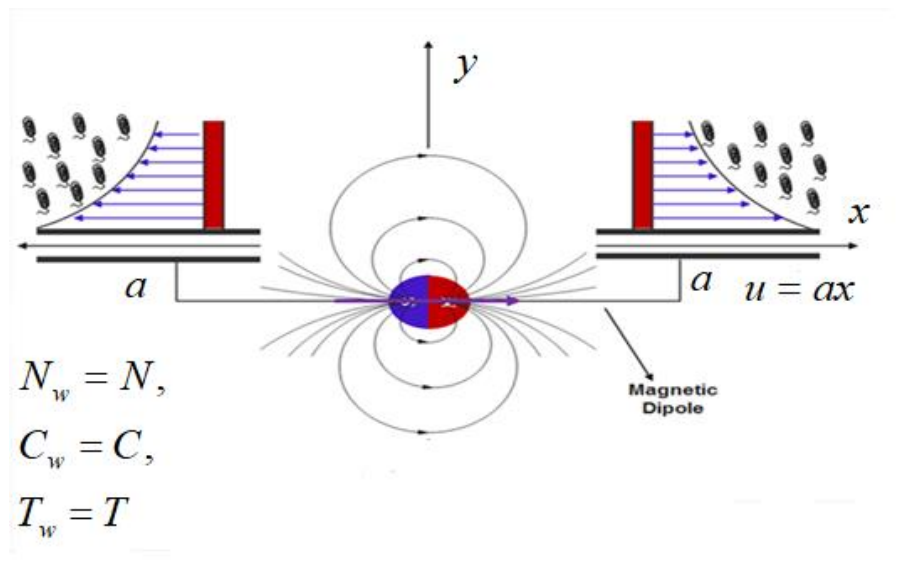
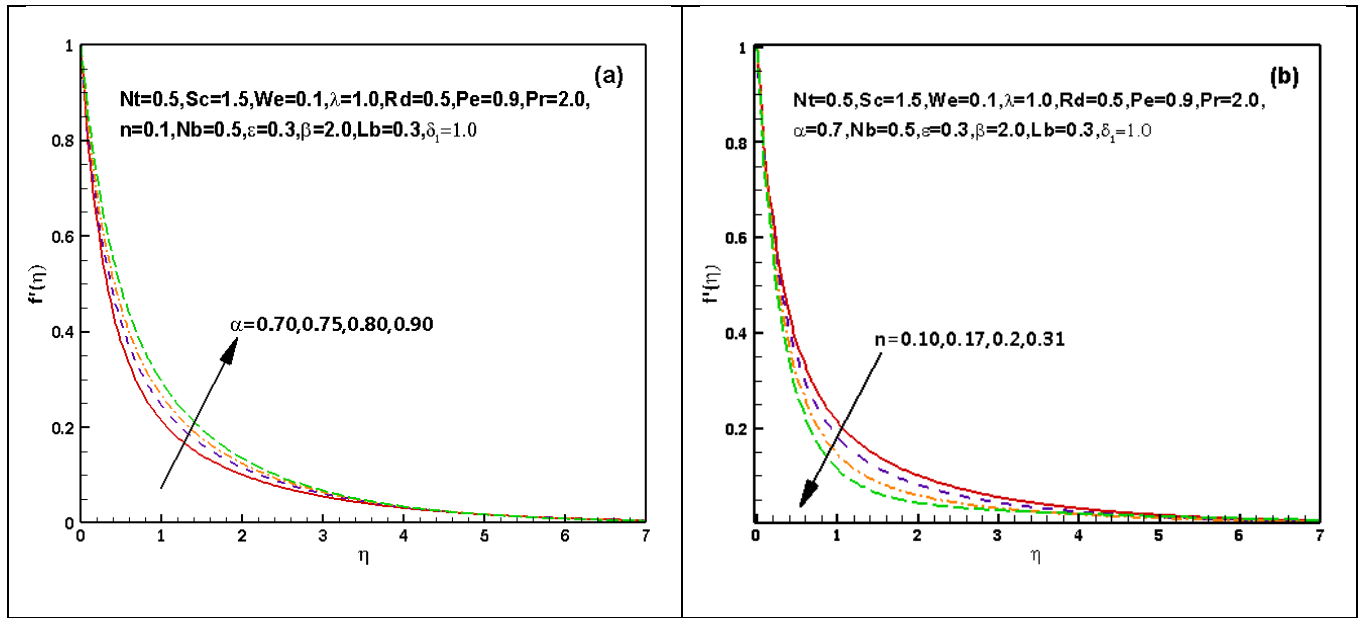
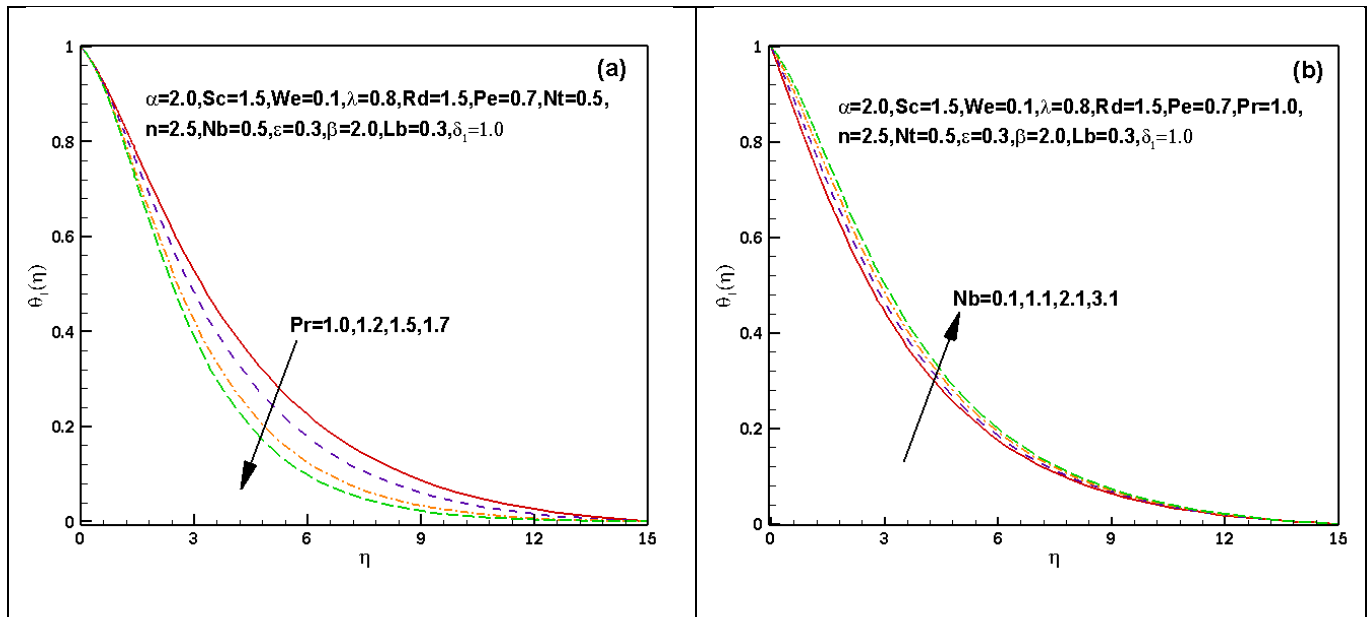


Fig. 1: Systematic Diagram.

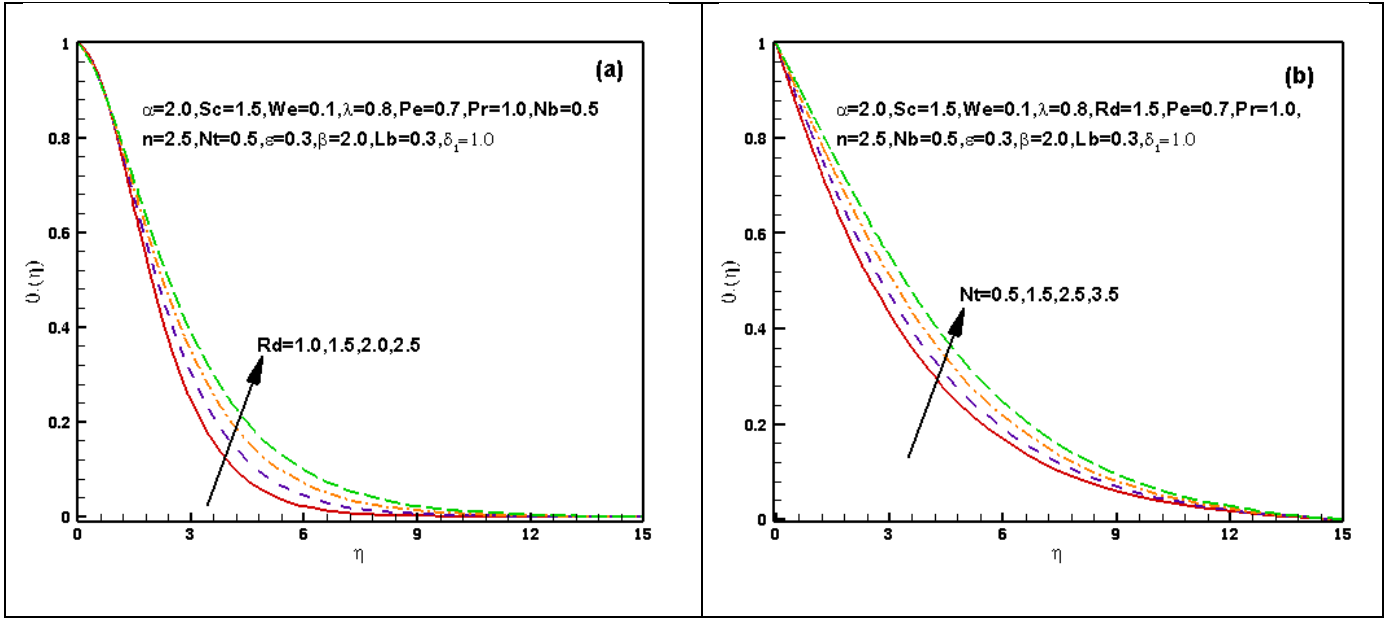




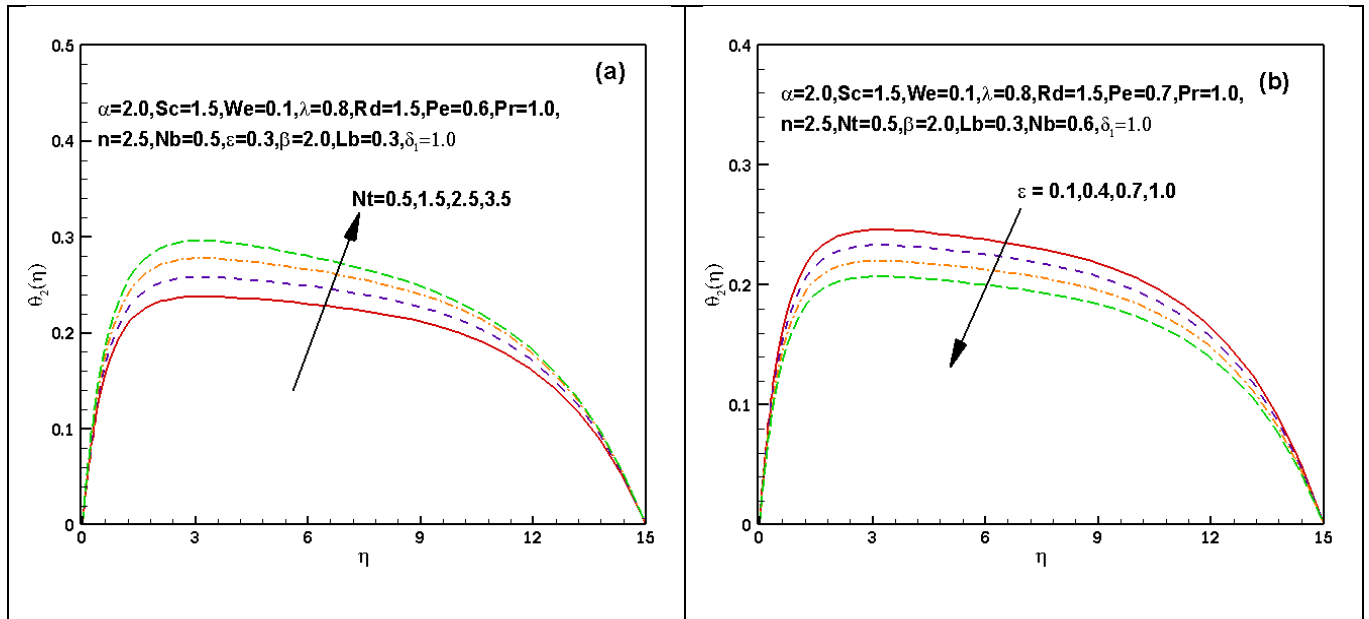
Figs. 2(a, b) Outcome of diverse values of  $[\alpha]$  and power law index  $[n]$  on  $f'(\eta)$ .



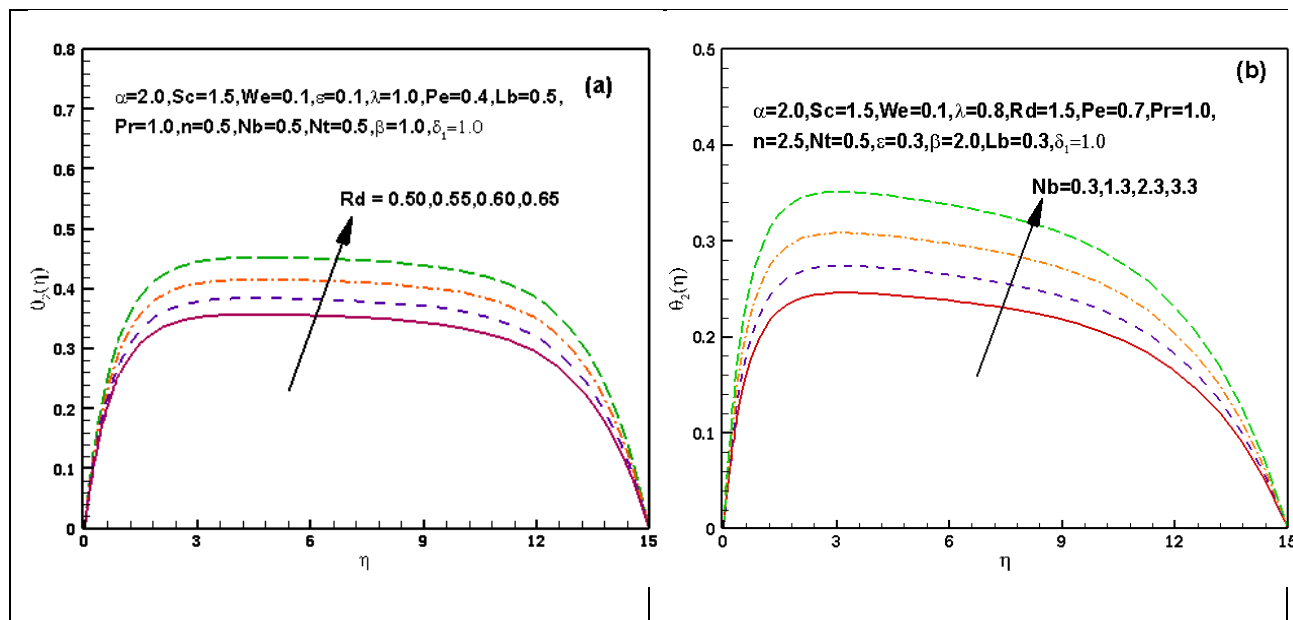
Figs. 3(a, b) characteristics of  $[Pr]$  and  $[N_b]$  on  $\theta_1(\eta)$ .



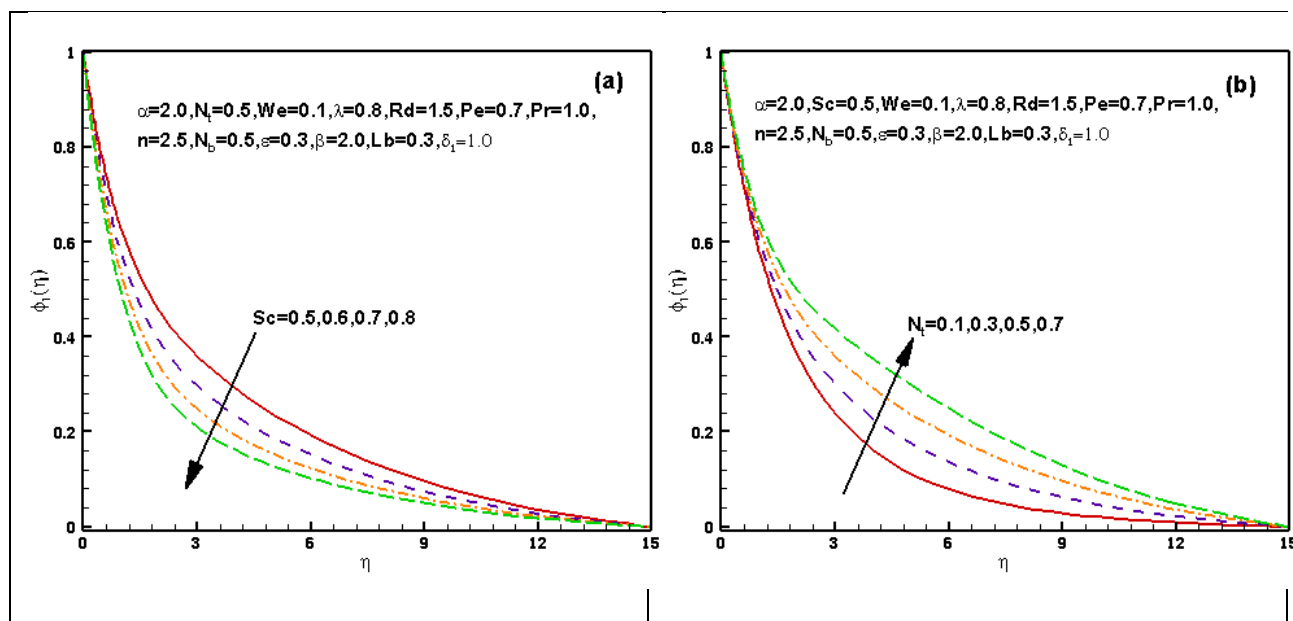
Figs. 4(a, b) impression of dissimilar estimations of  $[Rd]$  and  $[N_t]$  against  $\theta_1(\eta)$ .



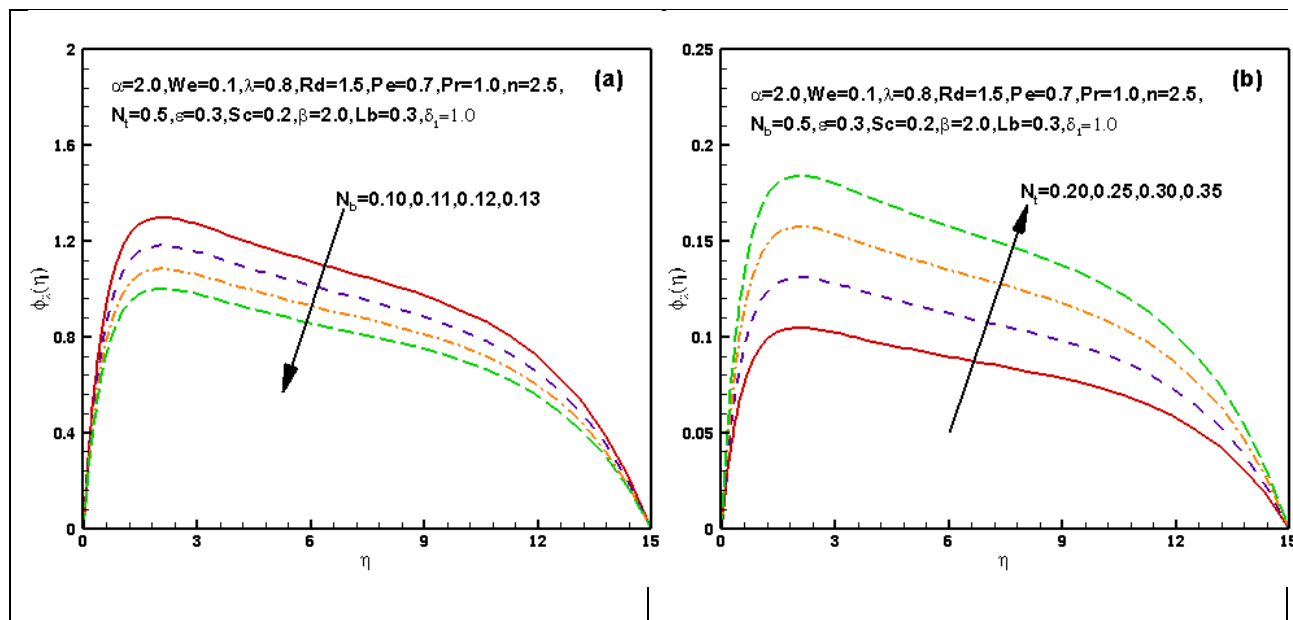
Figs. 5 (a, b) Impact of different values of  $[N_t]$  and  $[\varepsilon]$  on  $\theta_2(\eta)$ .



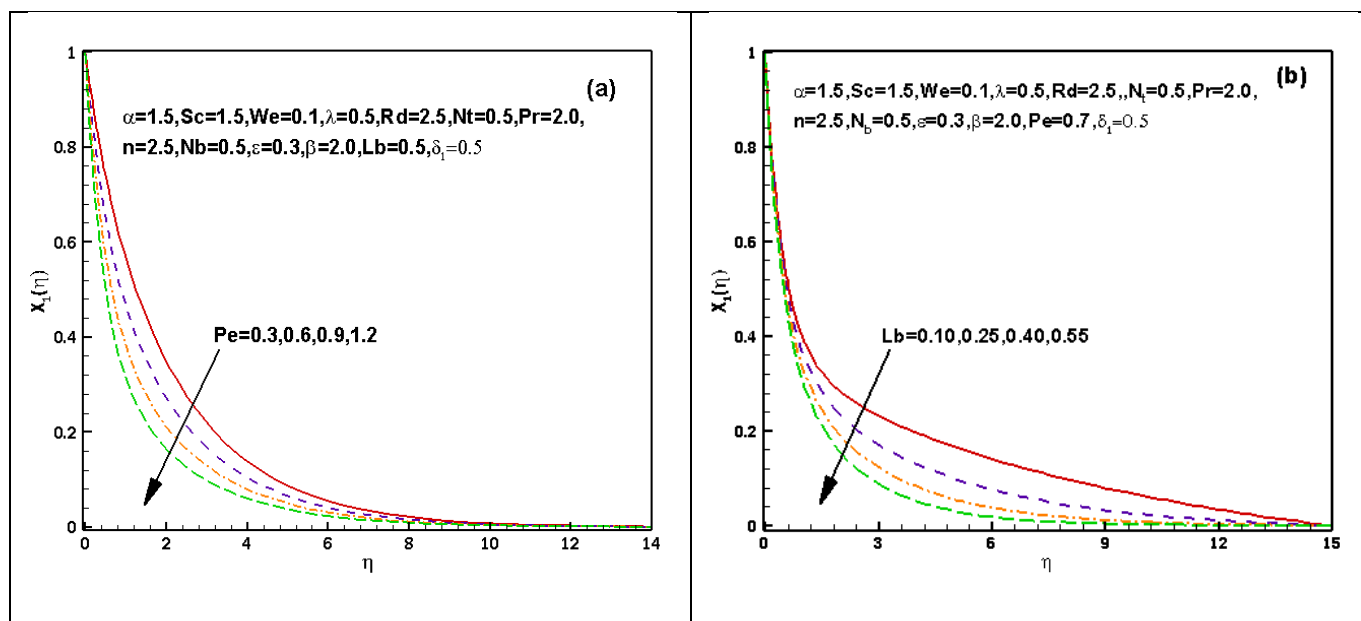
Figs. 6(a, b) Aspects of different values of  $[Rd]$  and  $[N_b]$  against  $\theta_2(\eta)$ .



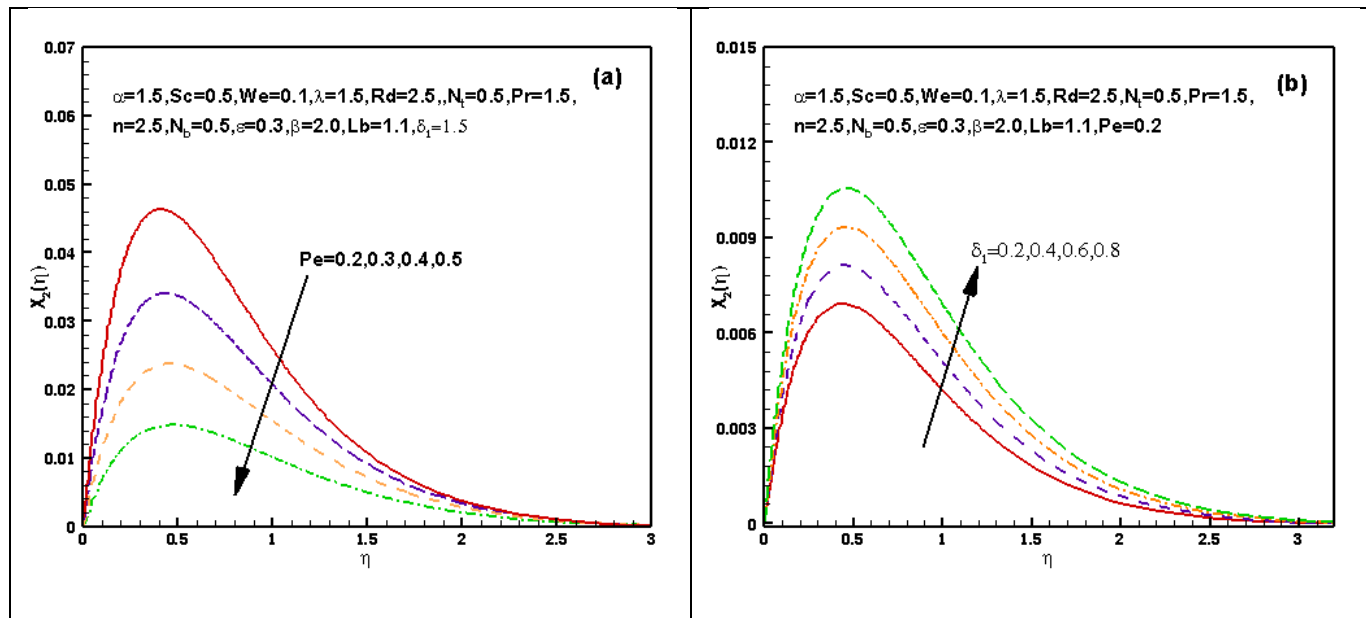
Figs. 7 (a, b) influence of diverse effectd  $[Sc]$  and  $[N_t]$  on  $\varphi_1(\eta)$ .



Figs. 8 (a, b) impact of different  $[N_b]$  and  $[N_i]$  on  $\phi_2(\eta)$ .



Figs. 9 (a, b) Consequences of  $[Pe]$  and  $[L_b]$  on  $\chi_1(\eta)$ .



Figs. 10 (a, b) Consequences of  $[Pe]$  and  $[\delta_1]$  on  $[\chi_2(\eta)]$ .